10 May 1984, 9:00 am - 12:00 pm

The Stability of Underground Power Chambers in the Brittle Rock

Weishen Zhu
Institute of Rock and Soil Mechanics, Academia Sinica, Wuhan, China

Kejun Wang
Institute of Rock and Soil Mechanics, Academia Sinica, Wuhan, China

Guangzhong Peng
Institute of Rock and Soil Mechanics, Academia Sinica, Wuhan, China

The Stability of Underground Power Chambers in Brittle Rock

Weishen Zhu

Associate Professor, Institute of Rock and Soil Mechanics, Academia Sinica, Wuhan, China

Kejun Wang, Guangzhong Peng

Assistant Professor, Institute of Rock and Soil Mechanics, Academia Sinica, Wuhan, China

SYNOPSIS The statistical analysis has been executed for the phenomenon of disk cores in the dam site, which has been compared with the condition of high geostresses. The mechanism to form disk cores and the stress state and energy distribution around underground power houses have been analysed with FEM. In addition, the modelling test to investigate the stability of underground house with block material is introduced. Finally some practical conclusions are proposed.

The Ertan Hydropower Station will be located in the remote mountain and gorge region of the Ya-long River in South-west China. The rock mass in this region is rather hard and intact and the scope of fault is small. The rock strata consist mainly of basalt and deuterogenously intrusive syenite. Along the banks of the dam site are high steep mountains (about 400-500m) with an average slope of 30 to 40 degrees. The height of the dam and the storage capacity of the reservoir are 245m and $5.8\times10^9 m^3$ respectively by estimate. The installed capacity of the station is 3-3.5M.KW. The underground power house with a length of 240m, a width of 27.5m, and a hight of 65m will probably be built near the abutment on the left bank. The feasibility of the power station project is being under consideration. In this paper, some research work on the stability of the underground power house is presented. The location of the underground chambers in the dam site is shown in Fig. 1.

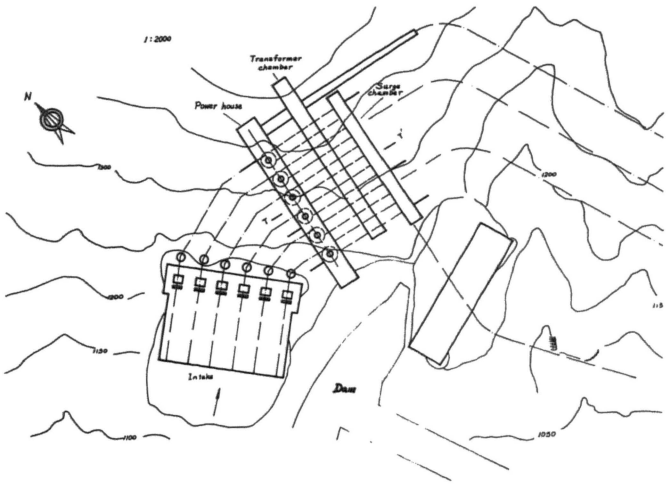

'ig. 1. Layout of Underground Power Chamers at Dam Site

. BRITTLE FRACTURE OF ROCK MASS AND HIGH ROCK STRESS

During the exploration stage of the project, nearly 200 prospecting bore holes with a total length over 20,000m were drilled in order to make engineering geology conditions clear. There are up to 84 bore holes in which phenomena of disking fracture of cores occurred, and 45 holes of them (53.6% of the total number) are situated in the lower parts of the river bed and the valley slope. The fracture surfaces are generally perpendicular to the axes of the bore holes. Rupture phenomena took place zonally and alternatively at various depths in every bore hole.

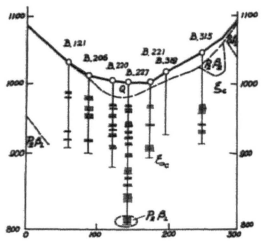

Fig. 2. Location of Disk Core

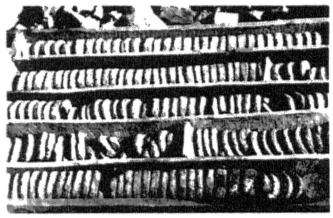

Fig. 3. Disks Formed in Succession

Fig. 2 shows the distribution of disk cores in the form of bands in each bore hole located in the valley. The average thickness of these rock disking bands is about 0.2-0.5m. The thickest band has a total length of up to 13.53m, in which 500 disks formed in succession (Fig. 3).

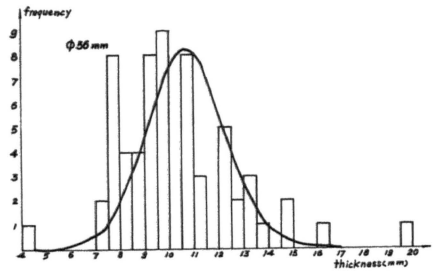

Fig. 4. Probability Distribution of Disk Thickness for Bit of ϕ56mm

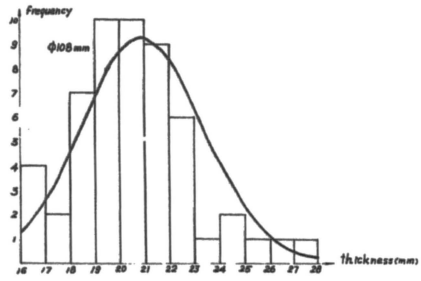

Fig. 5. Probability Distribution of Disk Thickness for Bit of φ108mm

The average thickness of the rock disks, h, is d/4 to d/3 (d—diameter of a core). Fracture surfaces are often fresh and rough. The top surfaces of the disks are concave and the bottom ones are convex, their thicknesses are generally proportional to their diameters. The statistic analyses have been done to 74 rock disks overcored from boreholes of φ56mm using diamond bits and 58 disks from φ108mm boreholes, the distribution probabilities of disk thicknesses are shown in both Fig.4,5. Their average thicknesses are 10.67mm (for φ56mm boreholes) and 20.86mm (for φ108mm boreholes) while the diameters of the cores are 38.8mm (for the former) and 81.8mm (for the latter). The ratio of h/d are 0.275 and 0.257 respectively. The statistical distribution of 332 fracture bands of 54 boreholes along the altitude of the river valley is shown in Fig.6. From the figure, it can be seen that

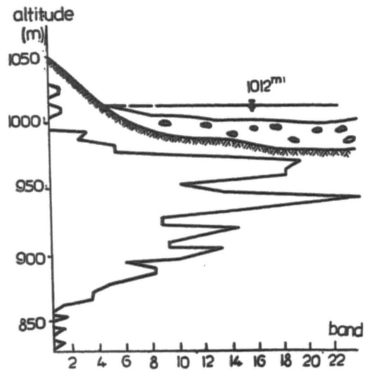

Fig. 6. Distribution of Fracture Bands along the Altitude of Valley

higher fracture probability appeared at the altitudes between 930—975m making up 74.7% of the total number. And at the altitude between 930—975m, there exists the highest probability. This band is 20—40m just underneath the surface of the rock base. According to the results of a series of experiments and analyses, it can be defined that the main contributing factors of disk phenomena are the stress concentration at the bottoms of the cores and partial unloading during the drill process in high level stress region rather than others such as tectonic,primary or mechanical movements of bits.

Statistical data from the disk bands have also shown that disking rupture phenomena mainly occurred in syenite (amounting to 80% of the number of the whole bands). Therefore, series of laboratory tests for syenite samples have been performed on a servo-controlled rigid machine, the test results have indicated that almost all syenite samples made intensive burst sounds with flying out broken pieces when failure occurred. These tests were monitored by AE, the AE frequency curve is shown in Fig.7.

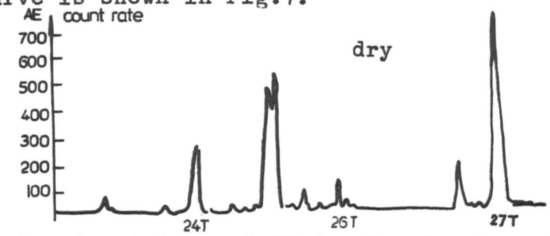

Fig. 7. Count Rate of AE for Dry Sample under Loading

A number of field measurement have been done in 33 measurement points by means of various overcoring methods and numerous data about stress distribution indicate that the orientation of the max principle stress with a magnitude of 250—300kg/cm at the location of power chambers near the left bank is NE 30° or so. Stress distribution is intensely affected by topography. From the slope surface of the valley to the deep part of the mountain, the stress distribution can briefly be diveded into 4 zones: (I) stress relaxation zone, (II) stress transition zone, (III) stress concentration zone, (IV) stable stress zone. The max principle stress measured at the 30—40m depth under base rock of the river bed may be up to 650kg/cm² . The regular stress distribution mentioned above can be seen in Fig.8. After reviewing Fig.8, one can see that concentration bands of disk core phenomena(Fig.6) are just corresponding to the high stress concentration bands at the river bed (Fig.8). The da-

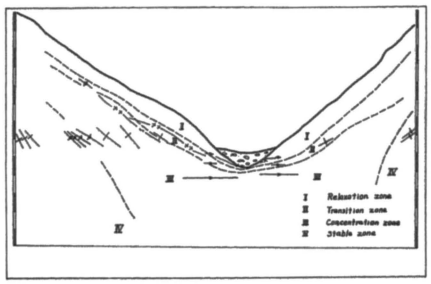

Fig. 8. Distribution of Rock Stress Divided into Different Zones

ta just mentioned lead us to conclude that the project is located in a region where there exists a high earth stress and the rock mass has obvious brittleness. Therefore, it is very important to make clear the fracture mechanism of rock disks and to predict the factors resulting in probable unstability of underground power station in order to take correspondent measures during design and execution of the project.

2. FEM ANALYSES

A, Fracture Mechanism of Disking

Three dimentional FEM analyses have been done to analyse the mechanical mechanism of disking fracture. The procedure of stress changes during drilling was simulated in the analyses using GJP—1 computer programme of our institute in

which isoparametric elements with 20 nodes were adopted. The process of simulation is shown in Fig.9. The max stress value measured at the river bed, namely, 650kg/cm² along X, 290kg/cm² along Y, was given as initial stress in calculation. Calculation was performed for situation without central boreholes of cores. The depth for each drilling was 3cm. Fig.10 and 11 illustrate the max tensile stress and max shear stress along symmetrical axis ABC (X axis) at level 5—5 and 4—4 as well as the directions and the magnitude of each pair of principle stresses at the X—Z plane when drilling reaches to the depth of level 5—5. From these two figures, it can be seen that there are rather high compressive and shear stresses(over 1000kg/cm² and 600kg/cm² respectively) at the root of the core, but tensile stresses only at the center parts of the cores. Therefore, it must be shear fracture if the fracture takes place along the periphery. At the same time, there are lower shear stresses and higher tensile stresses at the section B—B', especially at the periphery of the core, the tensile stress is up to 250kg/cm² which is much higher than the tensile strength of the rock($\sigma_t \doteq$ 80kg/cm²). In addition, from the stress-ellipsoid, one can find a tensile stress angle (about 30°) towards the center of the core. This will give an interpretation why rock disks are concave at top and convex at bottom in shape. This distribution of tensile stresses along the periphery of the whole core with the advance of drilling to different depths is shown in Fig.12. It can be seen from the figure that the stresses at the roots of the core are compressive while a sudden transition to a peak of tensile stresses takes place at the upper level and an abrupt reduction of tensile stresses occurs at the much upper level. According to the above analyses, therefore, the fracture of cores is probably due to shear stresses when it takes place at their roots, however, at the same time, the other possibility of the fracture mechanism may be tensile one at the upper level from the roots of the cores.

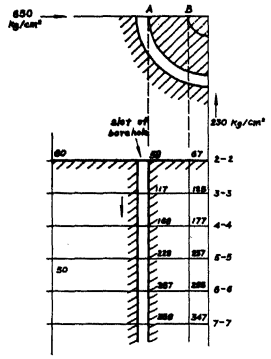

Fig. 9. Process of Drilling

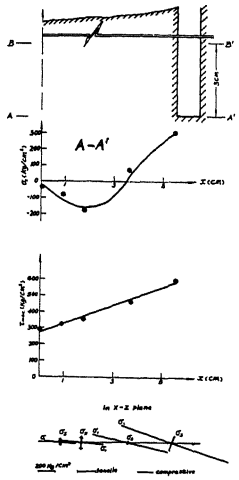

Fig. 10. Stress Distribution at A—A'

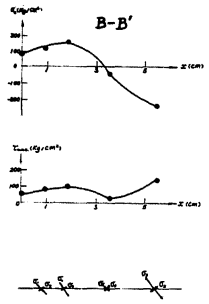

Fig. 11. Stress Distribution at B—B' section

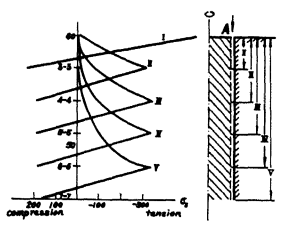

Fig. 12. Vertical Distribution of σ_3 at A at different drilling levels

B, Stress Analyses of Underground Power Houses

Because of large sizes of underground powerhouses and high earth stresses at the dam site, it is necessary to do FEM analyses. In consideration of hard surrounding rock and its good elasticity and closed joints due to high initial stresses, linear elastic analyses was performed at first. This kind of analysis, therefore, can be considered as one based on good similarities. GJP—1 computer programme was still introduced in calculation, isoparametrical elements with 8 nodes (for plane problems) and with 20 nodes (for cubic problems) were used for meshes. So far as the initial stress was concerned, an approximation by least square was introduced to process initial scattered data which were measured at the left bank of the river. This method made the stress state approximately coincident with both equilibrium and deformation equations. The comparison between two groups of stress values from the approximation by least square and from 6 measured points is illustrated in Fig.13, showing a good coincidence except individual components of specific points.

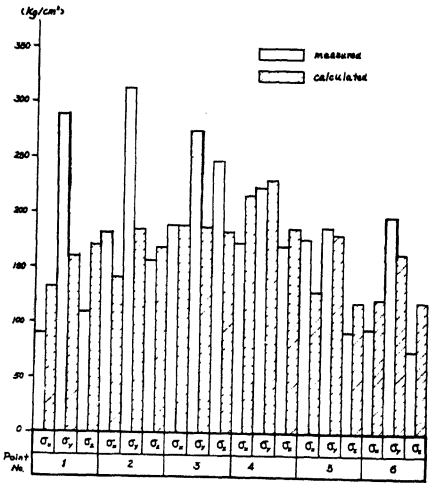

Fig. 13. Comparison of stress components between measured and calculated ones

Calculations were performed on three large openings, first by two dimentional analysis and then by three dimentional analysis. In order to overcome the specific computer's limitation of storage capacity, the whole space for calculation was divided into several subparts. Then, the results from each subpart were superimposed. As calculation scope concerned, the vertical sizes from upper and lower edges of caverns to fixed boundaries are twice as large as max height of the caverns, and the horizontal sizes

from two side walls of the caverns are seven times as wide as max width of them. The total number of the isoparametric elements and of the nodes were 265 and 1547 respectively in calculation. Dealing with the middle section of three

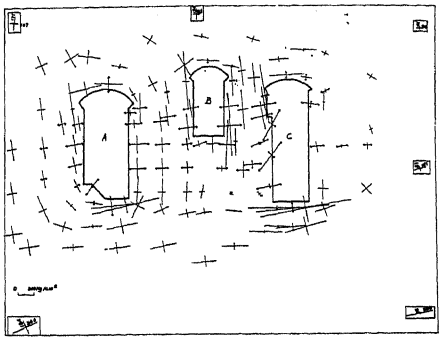

Fig. 14. Stress Distribution around Chambers in 3-dimentional Analysis for Section T-T'

dimentional analysis (Fig.14), one can see that most of the redistributed stresses are lower than the initial ones within the region surrounded by three openings to form a stress weakened zone because there is a high horizontal component more than 200kg/cm^2 in the stress field, especially, several tensile stress zones result around those openings and the most orientations of the stresses are approximately perpendicular to the peripheries of the openings. The width of the tensile zone at the left side of the main power chamber is nearly equal to that of this chamber, similarly, the width of the zone at the right side of the surge chamber is equal to the one of the chamber. There exists a high stress concentration at the corners of each opening. At the roof and floor of two side openings (A,C) there is a great compressive stress which is nearly parallel to the horizontal direction. The value of compressive stress at the roof of the openings reaches up to 400kg/cm^2 which is three times higher than the initial stress, while the stress value at the floor, especially for two larger openings, are four times higher than the initial stress, for instance, some local stresses for chamber A and C are 880kg/cm^2 and 1100 kg/cm^2. From the point of view of energy analysis, in general, there are obvious energy relief zones between those three openings and at the central parts of two outer side walls of openings(A,C), however, there are larger energy accumulation zones at some corners of the openings, for individual point the value of accumulation is ten times as high as the one before excavation at the left upper corners of openings B and C. Because of inhomogeneous initial stress field, both zonal energy accumulation and relief zones are irregularly distributed, which intercross each other. Considering the distribution of fracture regions(Fig.15), one can find that there are tensile-shear fracture zones with larger ranges at the left and right sides of openings B and C (strength parameters are rather conservative, which was given by designers (table I)). A fracture region with a certain range developed at the lower half of the left side wall and at the floor of opening A, in addition, there are several tensile-shear fracture zones at the roof and floor parts of openings B and C. It shoult be mentioned, however, that in three dimentional analyses was not considered the influences of galleries and tubes

TABLE I. Mechanics Parameters for Rock Mass

Parameters (in-situ)	Units	Syenite ($\mathcal{E}$)	Basalt (β)
E	Kg/cm^2	2×10^5	1.6×10^5
μ		0.15	0.20
γ	Ton/ m^3	2.7	3.0
σ_t	Kg/cm^2	10	10
c	Kg/cm^2	25	15
Φ	degree	65	57

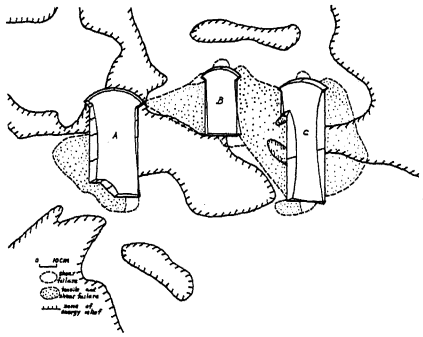

Fig. 15. Periphery Displacements, Energy Distribution, and Fracture Zones around Chambers for Section T-T'

near main chambers on stress distribution. For this reason, it can be predicted that the strength resistance ability of the rock will deteriorate owing to the existence of those galleries and tubes. This elucidates that corresponding measures in designing and constructing stage should be taken to improve the arrangement, shapes, and construction methods of the future underground chambers and so on to ensure the safety of this project.

3. PHYSICAL MODELLING TESTS

In previous paragraph, elastic FEM analysis on the stability of the rock mass surrounding three underground openings has been done. However, there exist widely three main joint sets in the rock mass of the left bank, of which sets NE and NW have a steep dip while set EW has a gentle one (Fig.16), these sets made rock mass become

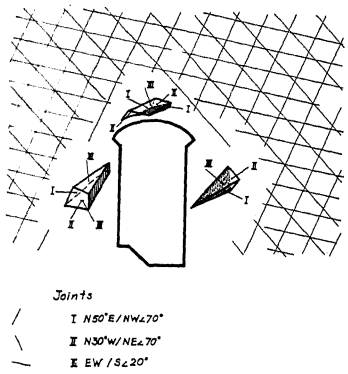

Fig. 16. Joint System around Power House

a complex comprising a great number of blocks (about $8\times5\times10m^3$). In order to take account of the influences of the joint on the stability of underground chambers, physical modelling tests have been performed according to similitude principles. The object of study is individual house at the present stage. For the purpose of simplicity, only sets NE and EW were simulated in test (Fig.17), this is because set NW has a smaller ratio of separation (<40%) and a short length of joints as well as because this study programme has a reference significance to the another design of power houses with location at the reservior due to the similar influences of joints orientation.

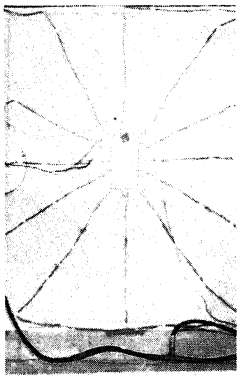

Fig. 17. Layout of Physical Modelling

A. Similitude Requisites

Model is satisfied for the similitude of the prototype, i.e. real situation under following aspects:

a, dimensions and shapes of engineering project
b, geometrical configuration of geological structure
c, physical and mechanical properties of rock mass
d, initial stress state
e, the sequences of constructions.

The sizes of model are 1.7m in height and 1.6m in width when ratio of 1/200 was chosen as the scale. A kind of mixture consisting of plaster, sand with different grading, and water can suffice the above similitude conditions of material. In Fig.18, a five-step excavation procedure simulating the real case is shown. For initial stresses, 288.4kg/cm² and 133.5kg/cm² are adopted as horizontal one(σ_1)and vertical one(σ_2).

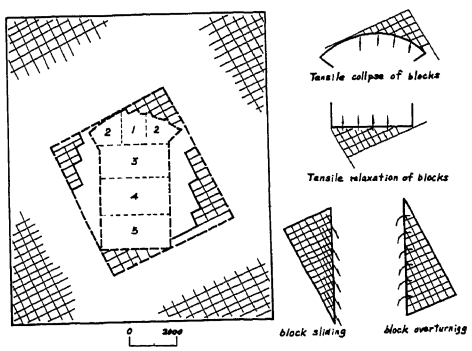

Fig. 18. Final Fracture Scale and Collapse type of Modelling

B. Deformation and Failure Character of Surrounding Rock

Vertical and horizontal stresses were exerted on the model to simulate the procedure of formation and transformation of rock resulting from overburden weight of rock and tectonic stresses. Afterwards, excavation was stepwise executed by five steps under constant loadings and deformation and failure of model were observed simultaneously which exhibited obvious regularities.

1) Character of deformation

(1) Both vertical and horizontal displacements were not marked at the bottom and top parts of the opening in the first step through the third one. In the cases of two side walls, vertical displacement was not marked, horizontal one is inward but value was small.

(2) During the fourth step through the fifth, the rock adjacent to the roof of the chamber had marked vertical outward (to rock mass) displacements having the max value of 0.1cm, while the rock of the bottom had rather small displcement. Obvious inward horizontal displacements, however, occurred at the two side walls, of which the max values for the lower reaches wall and upper reaches wall were about 0.3cm and 0.25cm separately. both of them occurred at mid points of these walls.

(3) After final excavating stage of the opening, the influence range of displacements was measured which reached to depth of 15cm measured from the top and 8.0cm from the bottom and 53.0cm and 52.0cm from the lower and upper reaches side walls (Fig.19), the horizontal range of displacement was eight times in total as large as the opening width.

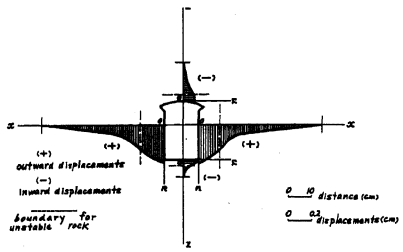

Fig. 19. Displacements Curves for Main Sections

2) Failure characters of rock

(1) There was no failure phenomena occurring from the first through the third steps with exception of collapses of some small triangle rock blocks surrounded by two joint sets and the open surface at the roof part of the opening during the second step.

(2) From the fourth step to the end of the fifth one, inverted sliding triangles surrounded by two joint sets and open surface at the side wall toward lower reach of the river formed. Inward upset along the joint with a steep dip and inward slide of blocks along the joint with a gentle dip occurred at the side wall toward the upper reach, while at the roof and floor of the opening presented tensile fracture along joints and structure loosen separately(Fig.18).

(3) The boundary of rock failure region is 11.4cm from lower reach side wall and 11.7cm from upper reach side wall and 1.5—2.0 cm from the roof

and 2.5–3.0cm from the floor of the opening (Fig.18).

3) The stability of the surrounding rock

(1) From the deformation and failure characters of the rock, it is known that surrounding rock will basicly be stable during the first through the third excavation step while it will become unstable markedly in the fourth and the fifth steps.

(2) In the case of the scope of deformation and failure of rock, it will reach farther parts from side walls than from both floor and roof of the opening, the former is twice as large as the latter.

(3) The types of unstability of surrounding rock are different, tensile fracture for roof rock, structure loosen for floor rock, sliding of rock blocks along the joint set of gentle dip with pull apart of steep joints for the rock at the side wall toward lower reach, and the upset along steep joint set and sliding collapse along gentle joint set for the rock at the side wall toward the upper reach.

(4) The sequences of occurrence of rock unstability: first one is at the side wall toward lower reach, second one at the side wall toward upper reach, and finally at the roof and floor of the opening.

(5) Because some simplicities, such as the ratio of separation assumed as 100% and substitution of two dimensional analysis for three dimensional one et al, are imposed on the prototype, the rock deformation, fracture, and its stability will differ from real situation to a certain extent. Nevertherless, the results of the model test will still offer an important reference because most of other factors strictly follow the principles of dimensional anlyses and similitude.

CONCLUSION

A. The phenomena of disk cores frequently occurring in boreholes in the dam site seem to result mainly from the rather high rock stresses and obvious brittleness of syenite in the region. The results from FEM analyses indicate that there exist a large shear stress at the roots of the cores and a high tensile stress at the parts about 3cm above the cores' roots, so two types of failure, i.e. tensile and shear ones may occur.

B. The results obtained from three-dimensional FEM analyses on the underground chamber group located at the dam abutment show obvious loosen areas with tensile stresses occurring in the neighbourhood of the outer side walls of the three chambers and at the region between the chambers, in other words, tensile-shear failure may occur. The results also show a large energy accumulation due to compressive stresses near the floor and the roof of the chambers. At the lower coner parts of the two large chambers, the compressive stress may be four times as large as the initial one. For this reason, protection measures should be taken at the bottoms to keep the rock from bursting.

C. From physical modelling test on joint rocks, it is known that the deformations of surrounding rock during the upper excavation of the opening are small, but they are becoming larger markedly during the lower excavation of it, the unstable extent of two side walls are much higher than that of the floor and the roof, and the side wall toward lower reaches is more unstabl than the wall toward upper reaches. This lead us to come to the conclusion that the corresponding protection measures should be introduced at the design and the construction stage

ACKOWLEDGEMENTS

Many data in situ were offered by the Institut of Power Survey and Design, Chengdu. A sistan in writing this paper was made by Mr. Zhu Zuod Mr. Geng Zhichao, Miss Fang Zhaoru, and Miss M Ziping. Mr.Zhou Yu and Miss Zhang Lijun took part in the modelling test.

REFERENCES

Bai, S., W. Zhu and K. Wang (1983), "Some Rock Mechanics Problems Related to a Large Under ground Power Station in a Region with High Rock Stresses", Proc., 5th Int. Cog. on Roc Mech., Melbourne. D. 271.

Shi, J. (1979), "Brittle Fracture of Rock at High Stress Region", Interior Report of Ins of Power Survey and Design, Chengdu.

Yuan, J., K. Wang and J. Yang (1983), "GJP-1 a Three-dimensional Computer Program", Rock a Soil Mechanics, Vol.4, No.1 P. 25, (In Chinese).

Sun, Z. (1983), "Preliminary Research on the E gineering Problem Fitting with Zonal Distri bution of High Stresses at the Ertan Valley Interior Report of Inst. of Power Survey ar Design, Chengdu.